ELSEVIER

Geomorphology 28 (1999) 201–221

GEOMORPHOLOGY

Alluvial fan and catchment initiation by rock avalanching, Owens Valley, California

Terence C. Blair *

Blair & Associates, 1949 Hardscrabble Place, Boulder, CO 80303, USA

Received 3 July 1998; received in revised form 29 October 1998; accepted 4 November 1998

Abstract

The North Long John alluvial fan of the Inyo Mountains piedmont, Owens Valley, CA, was catastrophically initiated by a prehistoric (early Holocene?) rock avalanche. This avalanche resulted from the collapse and disintegration of the central part of a 1.1×2.0 km range front bedrock facet comprising the divide between the catchments of two large, adjoining alluvial fans. Failure rapidly produced and transferred ~ 25 million m^3 of new sediment to the piedmont, where it was deposited in the trough between two coalesced fans. These deposits are of unstratified, angular, muddy, bouldery and cobbly pebble gravel present in a U-shaped form. This form consists of lateral levees 10 to 60 m tall that lead 1.6 km from the range front to a 108 + m high distal snout. The avalanche sediment comprise the initial platform for, and still dominate the nascent North Long John fan. Rock avalanche failure also created a 100 + m deep concave scar in the range front that now serves as the fan catchment. The slopes of this catchment are mantled by colluvial sediment generated from intense shear along the avalanche detachment surface. Thus, the avalanche served as an alluvial fan 'starter kit' by building the fan platform, and by creating a range front catchment lined with sediment. Because of this unique and recent origin, the North Long John fan and its catchment are in an early stage of development, lacking features such as old surfaces and a well-developed drainage net typical of the older, adjoining alluvial fans and catchments. Post-avalanche fan activity has been dominated by the deposition of ~ 4 million m^3 of sediment by debris flows. These flows, including one in 1984, were instigated by the concentration of flashy thunderstorm precipitation across the colluvium of the nascent catchment. Debris flows have built a conical tract that extends 1 km from the fan apex, and partially buries the older avalanche deposits. The debris flow tract consists of muddy, pebbly, cobbly, boulder gravel in levees 50–200 cm tall in the steep (12–16°) upper segment, and boulder-free lobes in the lower-sloping (5°) distal segment. This tract terminates in a 'pond' behind the avalanche snout, where recessional debris flow pebbly mud has been trapped. This pond eventually filled and was breached by a deep channel that now transects the snout of the rock avalanche. A second debris flow tract 300 m in radius has prograded outward from the end of the avalanche bypass channel. The facies of this tract are identical to those of the proximal fan. An abundance of colluvial sediment mantling the steep slopes of the catchment indicates that the North Long John fan will continue to enlarge by thunderstorm-induced debris flows.

Keywords: alluvial fans; rock avalanches; Owens Valley, California

* Tel: +1-303-499-6005; Fax: +1-303-499-6087; E-mail: tcblair@aol.com

0169-555X/99/$ - see front matter
PII: S0169-555X(98)00111-1

1. Introduction

Alluvial fans and fan catchments are common in tectonically active regions because of the development and maintenance of steep, fault-bounded range fronts with several kilometers of relief. Fan catchments typically originate and, thus, are focused on geological discontinuities in the uplifted block, such as faults, fracture zones, and geological contacts (Blair and McPherson, 1994a,b). Catchments arise in these naturally predisposed sites because of higher rates of physical and chemical weathering promoted by tectonic fracturing and water transfer. Erosion of sediment from these zones creates depressions that naturally focus surface drainage, in turn promoting more weathering and erosion, synergistically enlarging the fan catchment. Though rates of development may vary, these processes through time produce multiple, coeval catchments with matching alluvial fans that line the transverse margins of linear range fronts, such as those along extensional basins (Fig. 1; Wallace, 1978; Bull, 1984). The fans are the depositional sites for sediment eroded from the catchment, and transferred to the range front through the highest order channel of the drainage net called the feeder channel. The commonly ~0.5 to 3.0 km wide divides between the catchments comprise triangular bedrock facets at the range front (Fig. 1). The form of the triangular facets results from the erosional sloping of the sides of the catchment towards the respective feeder channels. The relief of both the catchments and facets will increase through time by continued fault offset and downcutting (Wallace, 1978; Bull, 1984).

The progressive development of a range front, especially increasing relief, may result in the instigation of a fan and fan catchment within the confines of a bedrock facet between two mature fan catchment systems. Such nascent 'facet fan' and catchment systems possess geomorphic characteristics different than the adjoining older fan systems, with important implications for diachroneity between fans and fan surfaces, piedmont evolution, and potential geologic hazards. The purpose of this paper is to illustrate the existence of this poorly documented phenomenon by presenting a case study of a bedrock facet fan and catchment initiated about 10 Ka BP by a catastrophic rock avalanche. This feature, called the North Long John fan, is located within the mature Inyo Mountains piedmont of Owens Valley near Lone Pine, CA (Fig. 2). The methods of study included: (1) describing and mapping the form and facies of the deposits using an enlarged aerial photograph base, (2) measuring surface slopes with a clinometer, (3) analyzing the grain size of five representative samples, (4) constructing topographic

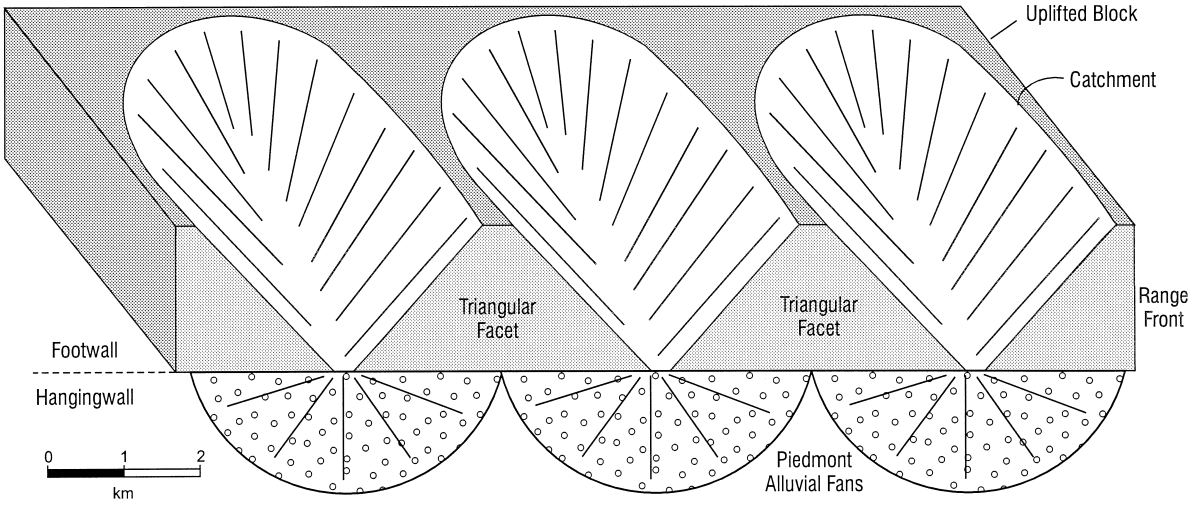

Fig. 1. Idealized fault-bounded range front and alluvial fan piedmont. Fan catchments are divided at the range front by bedrock triangular facets.

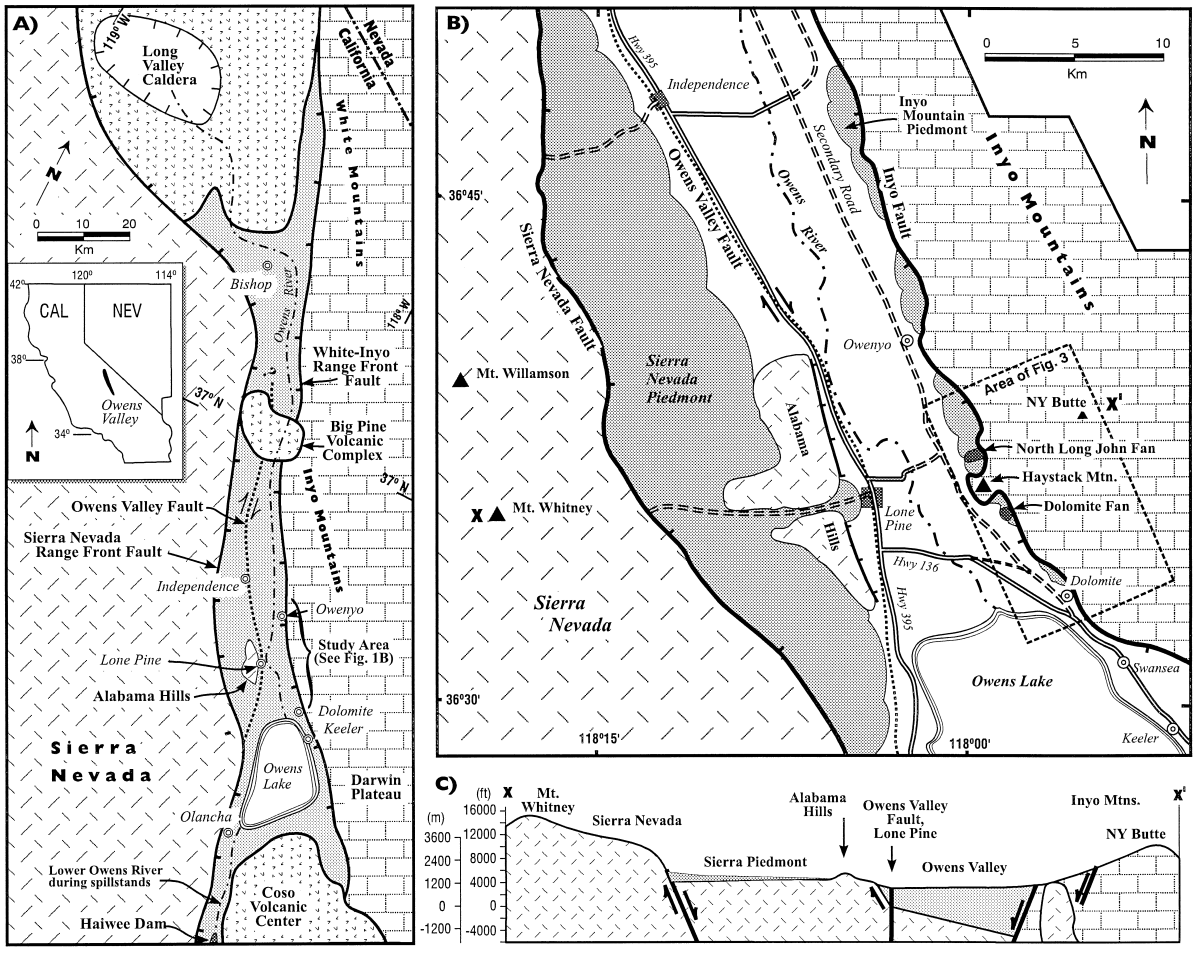

Fig. 2. (A) Geological features of Owens Valley, CA. (B) Map of southern Owens Valley, including the location of the ends of cross-section x–x' of (C), and the North Long John fan study area covered in Fig. 3. (C) Structural cross section x–x' between Mount Whitney in the Sierra Nevada through the study area to New York Butte in the Inyo Mountains (after Pakiser et al., 1964).

profiles and drainage nets using field data and U.S. Geological Survey 7.5′ quadrangles (scale = 1:24,000; contour interval = 10 m), and (5) comparing these characteristics with the older adjoining fans. Textural terminology used in this paper follows Folk (1974) as modified by Blair and McPherson (1999).

2. Setting

Owens Valley is a modern north–northwest trending rift 15 to 25 km wide and 150 km long located along the western margin of the Basin and Range province in California (Fig. 2). The basin is enclosed at both ends by Quaternary volcanoes, including Long Valley in the north and the Coso complex in the south. Owens Valley is precipitously bounded on the west, with 3200 m relief, by the Sierra Nevada, and on the east by the Inyo Mountains, with 2200 m of relief (Fig. 2). These margins are delineated by the active Sierra Nevada normal fault on the west, with >3500 m of throw, and by an equally prominent normal fault along the Inyo Mountains to the east (Pakiser et al., 1964). Additionally, a major oblique-slip fault called the Owens Valley fault cuts longitudinally down the basin along the east side of the Alabama Hills (Fig. 2; Pakiser, 1960). Both dextral strike slip (11 m) and dip slip (2 m) occurred

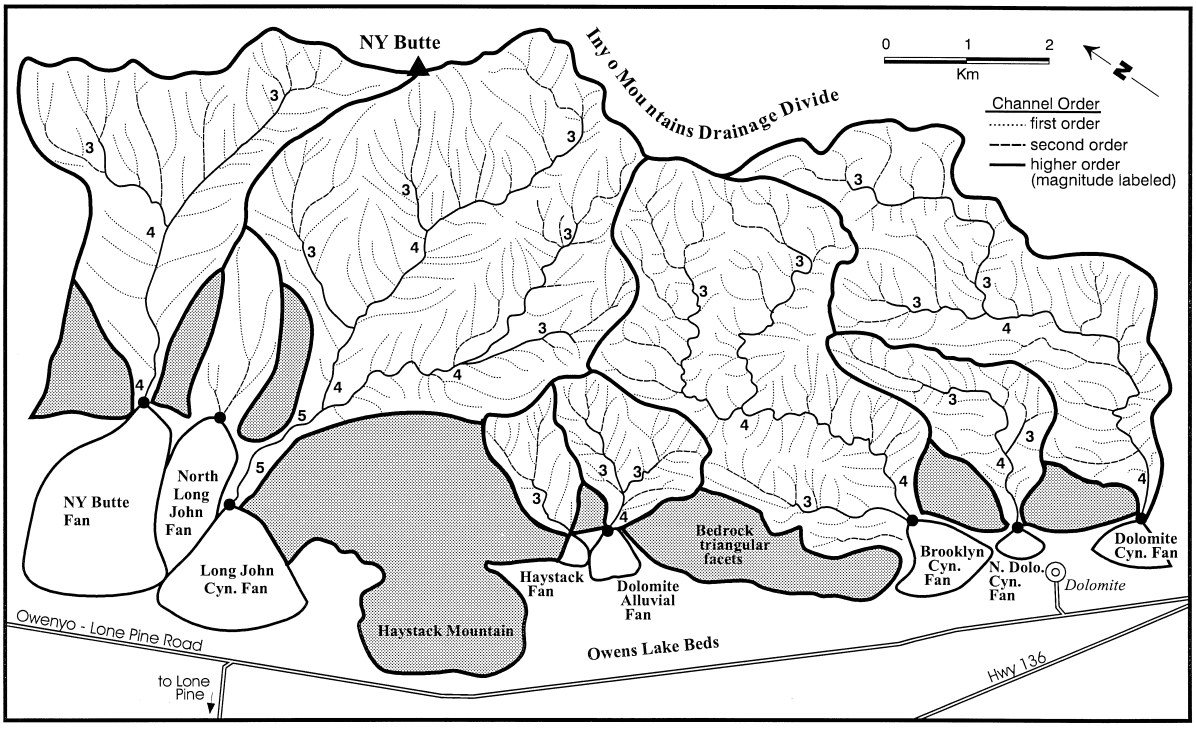

Fig. 3. Location map of the Inyo Mountain piedmont in the study area, including a detailed plan of the alluvial fans and the catchment drainage nets (see Fig. 2 for location). Drainage nets are based on the stream-order methodology of Horton (1945) and Strahler (1964), and use of 7.5′ U.S. Geological Survey topographic maps (scale: 1:24,000; contour interval: 10 m).

along this fault on 26 March 1872 during one of the largest (M ~8.3) historic earthquakes in the USA (Lubetkin and Clark, 1988). Basin development results from subsidence of the Owens Valley hanging-wall between this Owens Valley fault and the Inyo range front fault (Fig. 2). Gravity data indicate that the sedimentary fill thickens to 2500 m at the Inyo front, and outlines an east-tilted half graben (Pakiser et al., 1964).

Sedimentologically, southern Owens Valley is characterized by basin-marginal alluvial fans of the Sierra Nevada and Inyo piedmonts, and on the basin floor by the axial Owens River and Owens Lake system (Fig. 2). The alluvial fans have longer radii

Fig. 4. Features of the North Long John fan and catchment. (A) Overview of the 2200 m high Inyo Mountain range front and piedmont, including the North Long John fan (apex at middle arrow), and the adjoining New York Butte (apex at left arrow) and Long Canyon fans (apex at right arrow). Two prominent triangular facets are present, one north (A) and one south (B) of the New York Butte catchment. The North Long John fan catchment is developed within the latter facet. Also identified are the frontal snout of the rock avalanche (s), and a fault-backed bench along the south side of the catchment (b). (B) Close up of the colluvium-mantled catchment (c), downdropped bedrock facet bench (b), fan apex (arrow), proximal debris flow tract (below arrow), distal debris flow tract (d), and the 108 m high frontal snout (s) of the rock avalanche. Also marked are the New York Butte (N) and Long Canyon (L) drainages around the triangular facet. (C) Aerial photograph with features marked, including the apex (a), proximal (p) and distal (d) debris flow tracts, rock avalanche snout (s), lateral levees (l), back-avalanche pond (n), sinuous channel through the snout (c), and the sharp cut through older New York Butte fan deposits (arrows). The margin of the U-shaped rock avalanche is outlined. True width of photograph is 1.6 km. (D) Upslope view of the proximal debris flow tract (p). Light-colored deposits (arrow) are from a 22 August 1984 debris flow. Also visible is the avalanche scar (c) and the fan apex (a). (E) Upslope view towards the rock avalanche snout (s) showing the distal debris flow tract, including its apex (a) at the end of the snout-bypass channel.

(5–8 km) and lesser thickness in the Sierra piedmont, and shorter radii (typically < 2.5 km) and probably greater thickness in the Inyo piedmont. The basin floor is dominated by the 0.22° sloping longitudinal Owens River, which flows from its headwaters in the high Sierra Nevada and Long Valley volcano southward 100 km to its present terminus in Owens Lake (Fig. 2). Owens Lake is now a flat evaporitic playa formed by damming of the river by the Coso Range at the south end of the valley. Sedimentation is taking place in this valley under a high desert climate resulting from its position in the rain shadow of the Sierra Nevada. The valley floor is vegetated by alkaline scrub, including sage, grass, saltbush,

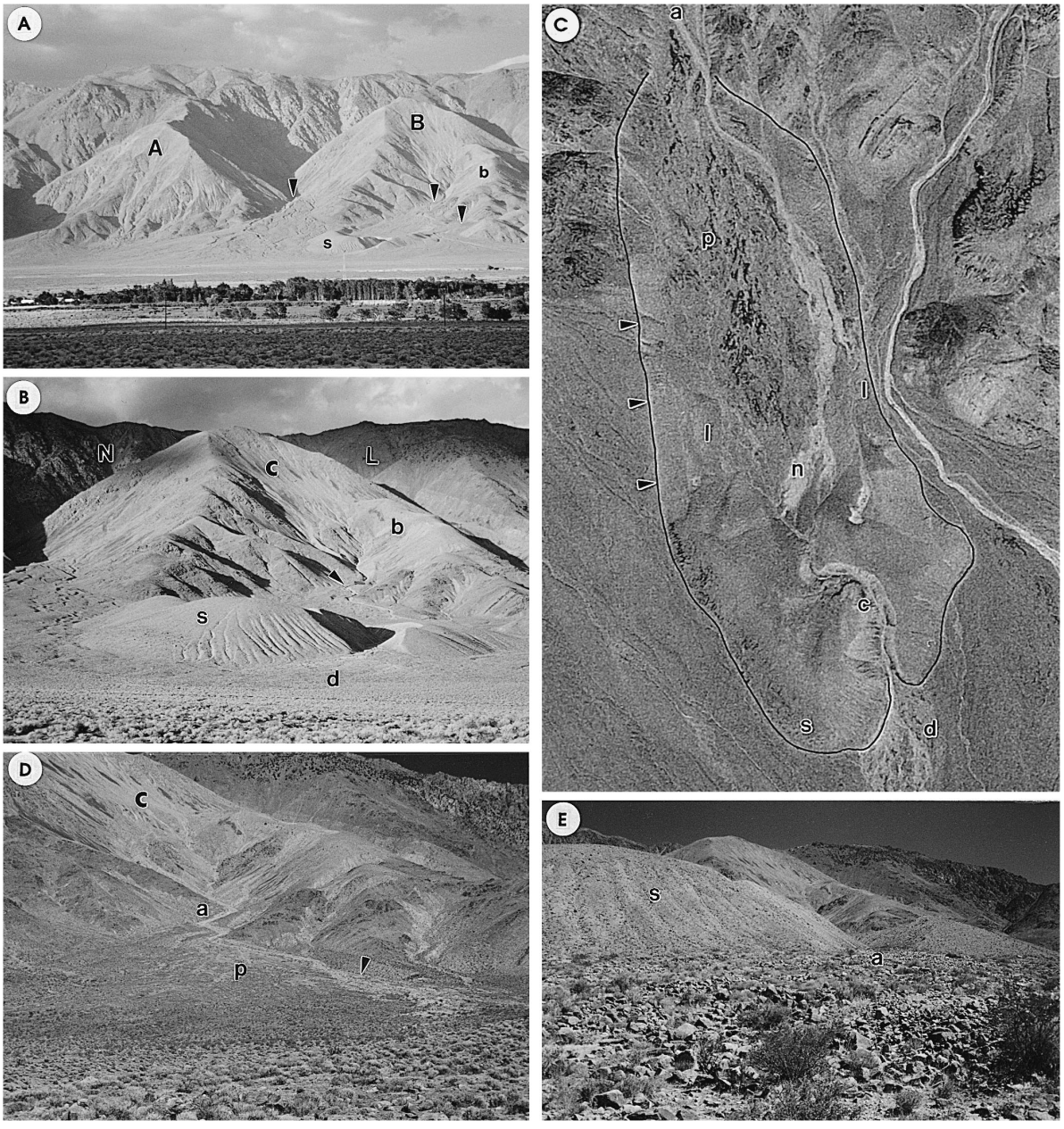

yucca, and cacti, whereas juniper and pinyon pine thrive in the adjoining mountains (Hollett et al., 1991). Annual precipitation varies with elevation from 10 to 20 cm, falling as rain and snow during the cooler months, and as local thunderstorms during the summer months (Hollett et al., 1991).

3. Morphologic overview of the North Long John fan and catchment

3.1. Catchment characteristics

The North Long John fan is located in the Inyo Mountains piedmont between the larger New York Butte and Long John Canyon fans (Fig. 3). The North Long John catchment is established in the prominent 2.0 km wide and 1.2 km tall triangular bedrock facet between the drainages of the adjoining fans (Fig. 4A). This catchment is a spoon-like concavity about 500 m in width, 50 to 100 m in depth, and with 1065 m of relief (Fig. 4B). It has an area of 2.0 km^2, and a poorly developed drainage net characterized by two second-order feeder channels (Fig. 3). The upper and medial parts of the catchment consist of 28 to 32° dipping slopes that are thinly mantled by colluvium (Fig. 4B). The 18° sloping lower catchment contains a thicker colluvial mantle, and has a rougher surface due to the presence of first-order rills. The catchment is bounded laterally by intact remnants of the bedrock facet. These remnants comprise 70 to 100 m thick benches downdropped 450 m from the facet crest along a sheared detachment surface (Fig. 4A). This surface is parallel to, and constitutes the northern extension of a normal fault along which Long Canyon is focused. Cretaceous granophyric aplite underlies the North Long John catchment, whereas Paleozoic sedimentary rocks and Mesozoic andesite underlie the adjoining New York Butte and Long Canyon fan catchments (Ross, 1967; Streitz and Stinson, 1974).

3.2. Fan morphology and provinces

The North Long John fan has an area of 0.83 km^2, relief of 270 m, and extends radially for 1750 m from the range front at an average slope of 8.8° (Figs. 3 and 5). Rather than having a smooth slope, the North Long John fan has an irregular composite morphology arising partly by its constricted position between the larger adjoining fans, but mostly because it consists of three provinces that have unique depositional origins. These provinces constitute a large rock avalanche that separates proximal and distal debris flow tracts (Fig. 4C–E). The rock avalanche tract has a U-shaped planview pattern 480 m across at the fan apex, and expanding to 640 m across at the terminus (Fig. 4C and Fig. 5). Paired lateral levees 30 to 50 m wide extend from the Inyo Mountain footwall for 950 m to the rock avalanche snout. This snout sharply terminates 1560 m from the range front. The height of the avalanche deposits above the adjoining fan surfaces is variable, increasing from 8 to 15 m in the proximal levees to as much as 108 m distally, resulting in a segmented longitudinal profile and a wedge-shaped radial geometry (Fig. 6). Besides a distal increase in thickness, this wedge shape also results from a lessening of surface slope from 15° in the proximal zone to 5° distally (Fig. 5). Cross-avalanche profiles consist of a double hump in the proximal leveed area, changing to a steep-sided blocky pattern in the distal snout (Fig. 6). Not including the inner courtyard above the snout and between the levees, this avalanche has an area of $\sim$500,000 m^2, most present in the distal levees and snout. A sediment volume of $\sim$25 million m^3 is determined for the avalanche by multiplying the area by thicknesses determined from field measurements (Fig. 5). Correcting for an assumed average porosity of 25%, this volume of rock avalanche sediment accounts for about 86% of the present volume of the fan catchment.

Rather than comprising continuous ridges, the paired avalanche levees consist of three definable segments 250–500 m in length, the most proximal two having a discontinuous relationship, and the distal two an overlapping relationship (Fig. 5). The three segments are delineated by differences in height and by discernible sharp boundaries. All three have surface slopes that decrease from 9–15° proximally to 2–7° distally (Fig. 7A). The lower two segments of the paired levees and the distal snout are separated by prominent, nearly vertical shear contacts that accommodated the downslope transfer of the avalanche (Fig. 7B). The progressive downslope offset of the more distal levees and snout from the

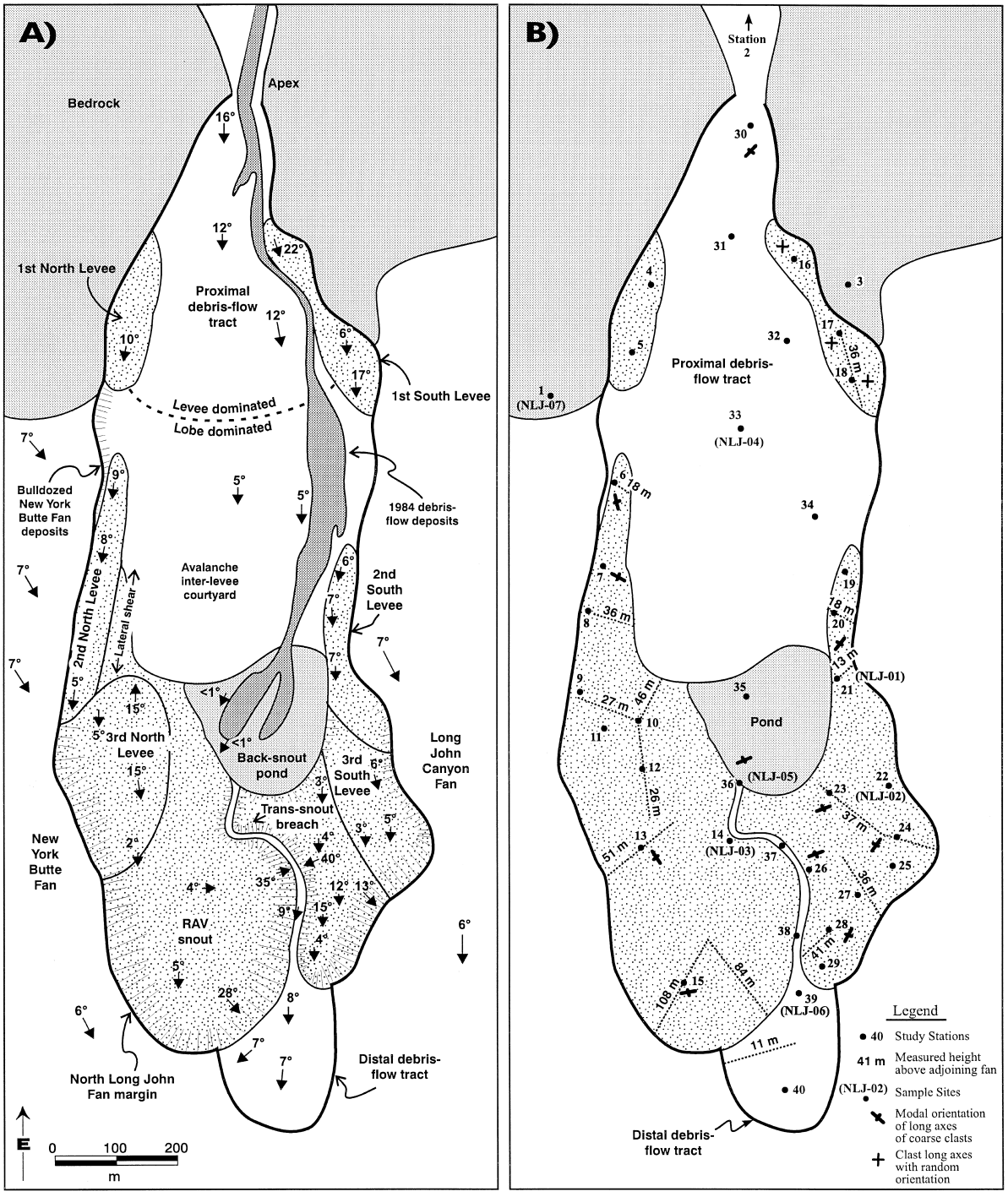

Fig. 5. (A) Components of the North Long John fan, and magnitude and direction of the slope of the surface. (B) Study stations, sample sites, measured thickness sites, and modal orientations of the long axes of elongate coarse clasts at given stations. Avalanche deposits in both maps are stippled.

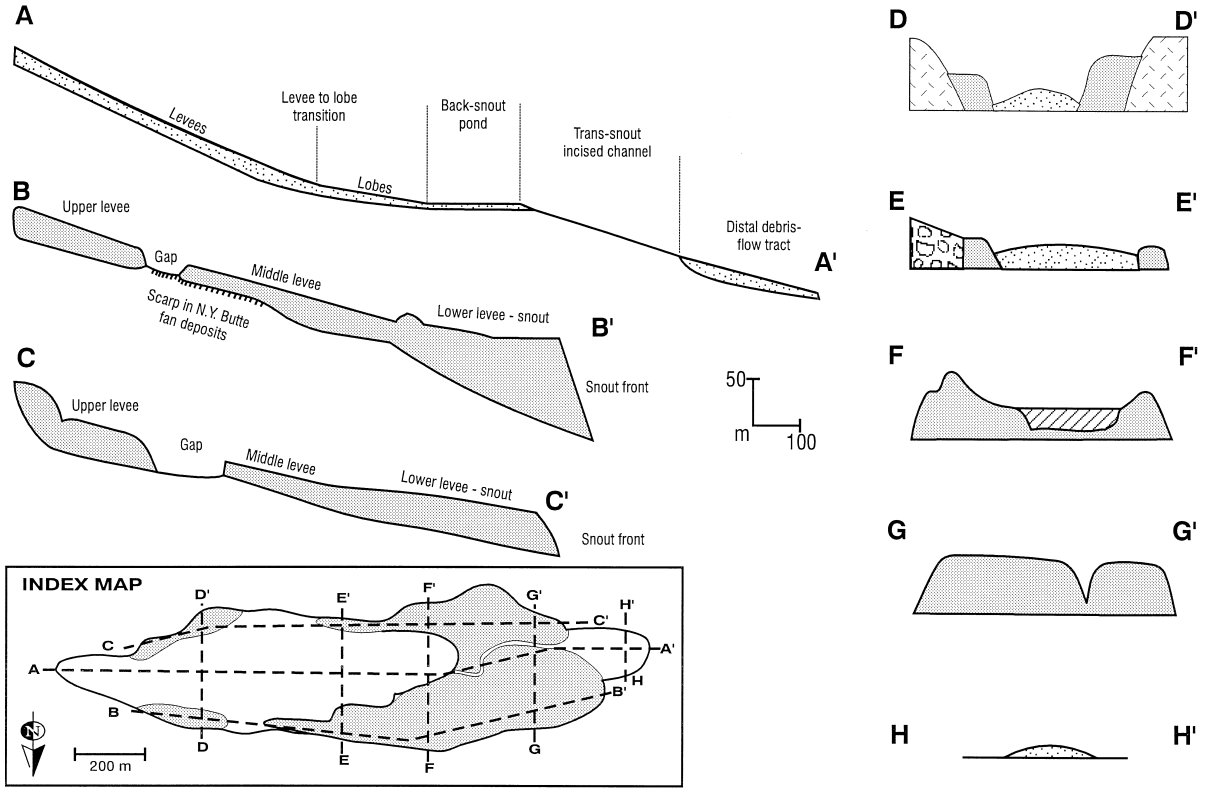

Fig. 6. Topographic profiles of the North Long John fan based on field measurements and contour maps. The rock avalanche deposits are shaded gray, debris flows are stippled, bedrock is cross-hatchured, the recessional pond has a diagonal pattern, and adjoining fan deposits have a gravel pattern.

inside margin of the upslope levee segments outlines a telescoped pattern between these elements (Fig. 5). The 2–5° surface slope of the snout is the lowest of the avalanche elements. This low slope abruptly changes at a brink point at the snout terminus, where the avalanche front descends as much as 108 m at a 28° slope (Fig. 4B). An ephemeral pond with a nearly flat, muddy surface 150 m long and 150 m wide is present immediately upslope from the snout and between the avalanche levees, produced by

Fig. 7. (A) Upslope view of the boulder-studded top of the northern levee, with the New York Butte fan to the north (a at apex). The long axes of the clasts have a slope-parallel alignment (e.g., arrows). (B) Downslope view of the second (2) and third (3) levee segments along the north margin of the rock avalanche. Sheared contacts, along which the third levee segment and snout deposits (s) were offset downslope, are marked with arrows. (C) Light-colored muddy sediment of the back-snout 'pond' (p) deposited by recessional flows from the proximal debris flow tract. The head of the channel (c) that transects the avalanche snout is visible. Rock avalanche levees laterally bound this zone. (D) Downslope view of the U-shaped planform of the rock avalanche, including the proximal end of the third levee segments (arrows), the distal snout (s), and the breached channel (b) through the snout. In the background are the town of Lone Pine (L), Alabama Hills (A) fronted by the Owens Valley fault, and the 3200 m high Sierra Nevada (S). (E) Vertical cut 5 m high of monolithologic megabreccia of the rock avalanche snout. The coarsest clasts are irregularly concentrated towards the top. (F) Close-up view of typical rock avalanche megabreccia texture consisting of unstratified, unsorted, clast-supported, very angular, muddy, sandy, cobbly, fine to coarse pebble gravel. The darkened zone above the 10 cm scale bar is a Bt soil horizon.

damming of the snout and the levees (Fig. 7C). The pond and avalanche snout are now breached by a prominent, sinuous channel extending from the pond to the southwest end of the avalanche (Figs. 5 and 7D). This 45 m deep, V-shaped channel is 5 m across at its bed and 20–50 m across at the snout surface. The channel walls typically slope inward 35–40°, whereas the channel bed slopes 9° westward.

The remainder of the North Long John fan consists of the two debris flow tracts. The largest one is developed on the proximal fan between the rock avalanche levees (Fig. 4D and Fig. 5). This tract is 300 m across and extends about 1 km from the fan

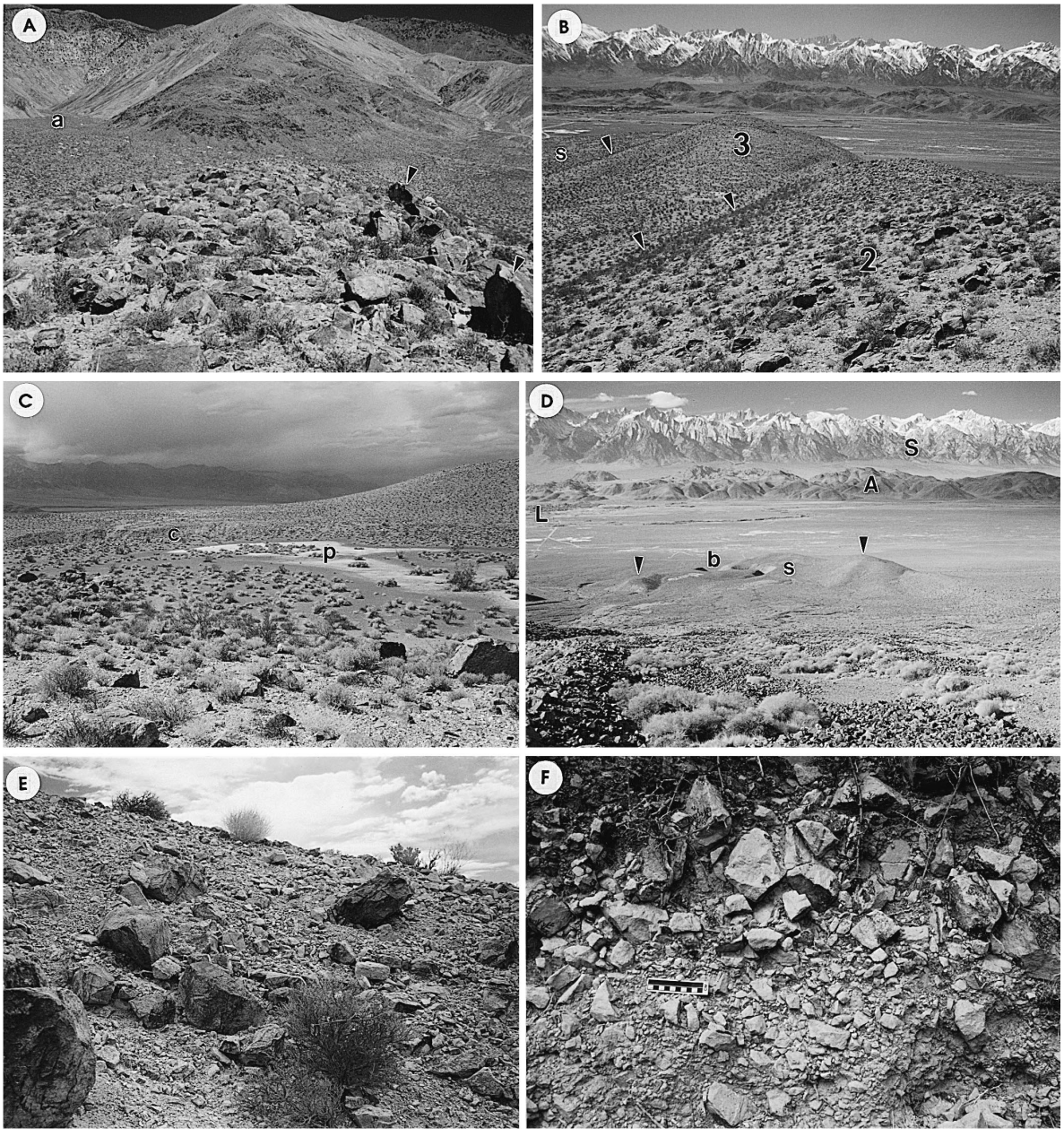

apex to the back-snout pond. It has an overall conical morphology that slopes between 12 to 16° proximally and ~5° distally, before merging with the nearly flat surface of the back-snout pond (Fig. 6A). The surface of this tract is rough where 1–4 m deep gullies are present, and smooth where a mantle of varnished angular boulders and cobbles is developed (Fig. 7D). The distal debris flow tract is 150 m across and 300 m long, commencing where the snout-bypass channel intersects the front of the rock avalanche (Fig. 4E and Fig. 5). Like the proximal tract, this distal tract has a conical form with a surface slope that slightly decreases distally from 9 to 7°. Overall, it is smoother than the proximal tract, with a slightly rilled surface of cobbles and boulders.

4. Rock avalanche facies and emplacement history

4.1. Rock avalanche facies

The rock avalanche deposits were described at 26 stations sited to cover all zones, including 10 in the northern levee, 10 in the southern levee, and six in the snout (Fig. 5). These deposits, whether of the levees or snout, dominantly consist of unstratified and unsorted, slightly bouldery, muddy, cobbly, fine to coarse pebble gravel (Fig. 7E–F). The clasts are monolithologic, consisting of tan to pinkish gray aplite identical to the bedrock underlying the catchment. The deposits mostly are clast-supported, and vary from tightly interlocking with abundant interclast long contacts, to loosely interlocking with tangential and floating grain contacts. These clasts have a diagnostic angular to very angular outline and dominantly are 2 to 8 cm across (Fig. 7F). The pebble-dominated, clast-supported texture becomes matrix-supported in the lower exposures of the avalanche snout. Particle size analysis of the < 1.6 cm ($< -4\phi$) fraction was conducted on two samples of rock avalanche sediment, including NLJ-02 from an upper levee site, and NLJ-03 collected from a lower snout exposure (Fig. 5). The data show these samples are extremely poorly sorted, and contain a full spectrum of sediment grades that include, on average, 58% pebbles and granules, 28% sand, 12% silt, and 2% clay (Fig. 8; Table 1). The clast-supported sample from the upper avalanche has a gravel–sand–mud ratio of 64–26–10 and the matrix-supported lower one 55–30–15 (Fig. 8).

Boulders and coarse cobbles overall are less common in the rock avalanche deposits than are pebbles and fine cobbles, and they lack a homogeneous distribution. Coarse cobbles and boulders are most abundant in the upper and outer parts of the deposits, where the sediment texture transitionally changes to an unstratified, angular to very angular, muddy, pebbly, cobble boulder gravel (Fig. 7E). Boulders commonly stud the surface of the avalanche levees (Fig. 7A). These clasts typically have an equant to bladed shape, and internally display crackle-breccia and jigsaw-breccia fabrics.

This coarsest fraction of the avalanche deposits was evaluated in greater detail by measurement of maximum clast size (intermediate axis, d_I), and the orientation of the long axes of the 10 largest elongate clasts, exclusive of those that have undergone post-avalanche movement. The d_I values range from 38 to 381 cm (fine to very coarse boulders) without any radial trend (Fig. 9). For example, the largest clast in the north margin of the rock avalanche (d_I of 300 cm) is present in the second levee segment, which is notably coarser overall than the proximal and distal levees at this margin. In contrast, the largest clasts along the southern margin (d_I to 381 cm), are in the distal snout (Fig. 9). Unlike maximum clast size data, the *a*-axis orientations of elongate cobbles and boulders are organized, displaying a moderately developed fabric at most of the study stations. The long axes of elongate clasts at the top and outer margins of the levee deposits are preferentially aligned either parallel to the trend of the levees or, more commonly, at about a 30° angle to this trend, with the inside end of the clasts consistently turned downslope (Fig. 5). A preferred elongate clast alignment also characterizes the snout deposits, with the modal trend generally oriented perpendicular to slope, paralleling the snout front (Fig. 5).

4.2. Reconstructed depositional history

The textures, fabric, monolithologic composition, and large-scale U-shaped lateral levee and snout morphology of the North Long John deposits are consistent with the products of a single large rock avalanche based on the similarity of these character-

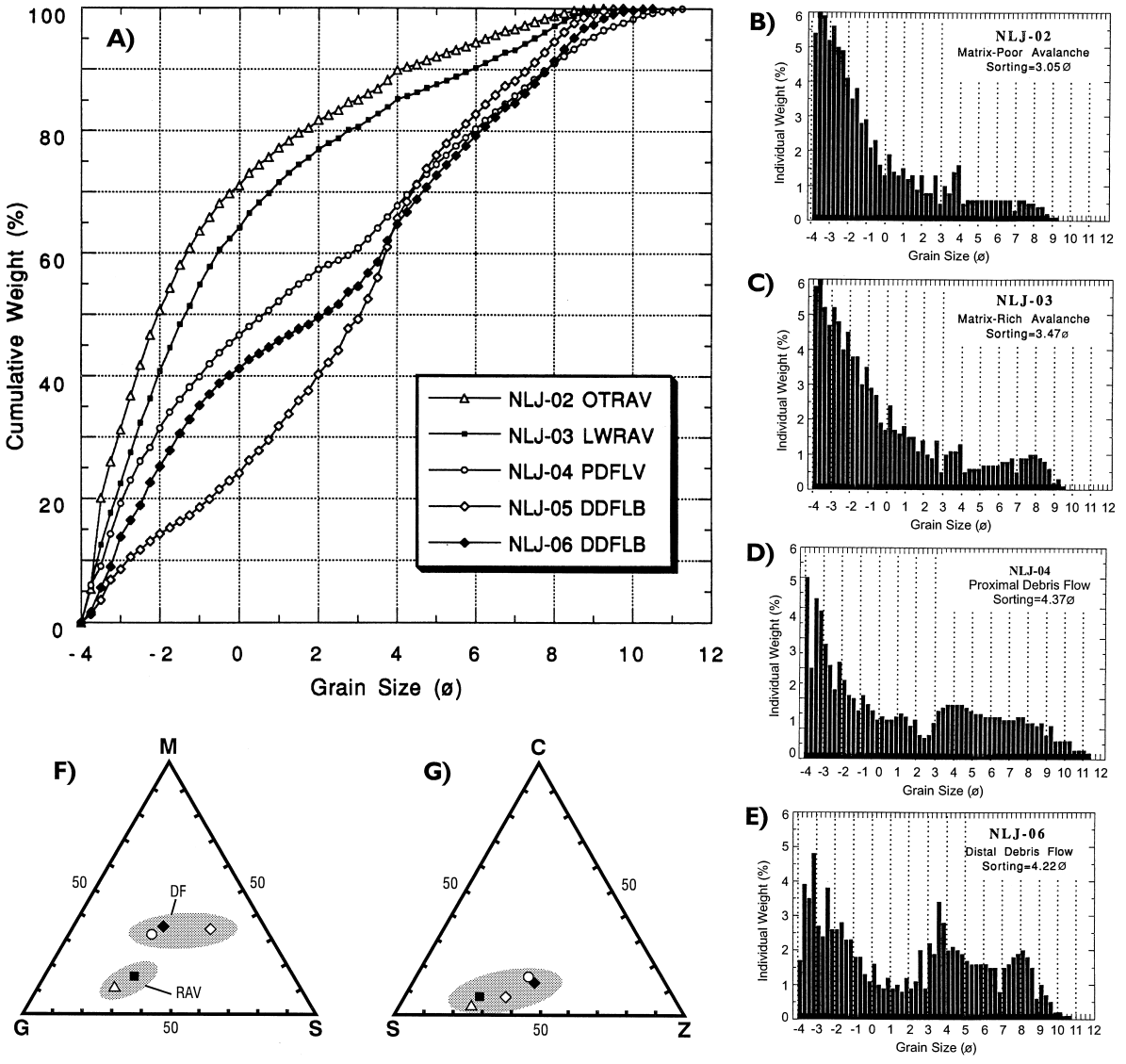

Fig. 8. (A) Cumulative curves based on grain-size analysis of two samples from the rock avalanche facies (NLJ-02 and -03) and three samples of post-avalanche debris flows (NLJ-04, -05, and -06). Sample sites are located in Fig. 5, and size-analysis data are summarized in Table 1. (B and C) Histograms of rock avalanche samples NLJ-02 and -03. (D and E) Histograms of debris flow samples NLJ-04 and -06. The mud content (finer than 4ϕ) in these samples is greater relative to the rock avalanche samples. (F) Gravel–sand–mud (G-S-M) ternary plot, and, (G) normalized sand–silt–clay (S-Z-C) ternary plot of the grain-size data from the five analyzed samples. Symbols are the same as those used in (A).

istics with those of historical rock avalanches (e.g., Hadley, 1964; Hsü, 1975; Gates, 1987), and with documented pristine deposits of prehistoric rock avalanches (e.g., Burchfiel, 1966; Shreve, 1968, 1987; Fauque and Strecker, 1988). The position of the proximal ends of the North Long John rock avalanche levees at the Inyo Mountain range front, and extending downslope from either side of the prominent range front bedrock scar, indicates that the avalanche was instigated by the catastrophic collapse

Table 1
Summary of grain-size data, North Long John fan samples

Feature/Smp	NLJ-02	NLJ-03	NLJ-04	NLJ-05	NLJ-06
Facies	OTRAV	LWRAV	PDFLV	PDFLB	DDFLB
Mode (ϕ)	−3.63	−3.63	−3.63	3.88	−3.13
Sorting (ϕ)	3.05	3.47	4.37	3.66	4.22
G-S-M	64–26–10	55–30–15	40–28–32	19–47–34	35–30–35
Nr S-Z-C	72–25–3	67–26–7	46–39–15	58–35–7	46–41–13
Grade	Weight percent of total sample				
m pebble	31.2	22.4	19.2	8.6	13.8
f pebble	19.5	18.4	12.3	5.7	11.4
granule	13.0	14.1	8.4	4.3	10.0
vc sand	7.4	9.3	6.8	5.5	6.0
c sand	6.1	7.4	5.5	7.7	4.6
m sand	4.6	5.4	5.2	8.5	3.8
f sand	3.3	3.7	3.5	9.0	5.0
vf sand	4.8	4.5	6.9	16.5	10.2
c silt	2.2	2.4	6.8	10.3	8.0
m silt	2.3	2.7	5.8	6.7	6.5
f silt	2.2	2.9	5.4	5.4	5.3
vf silt	2.2	3.9	5.3	6.4	6.9
clay	1.2	2.9	8.9	5.4	8.5

Smp—sample.
Facies: OTRAV—outer rock avalanche; LWRAV—lower rock avalanche; PDFLV—proximal debris flow levee; PDFLB—proximal debris flow lobe; DDFLB—distal debris flow lobe.
Sorting is Inclusive Graphic Standard Deviation (S_I) of Folk (1974).
G-S-M: gravel–sand–mud wt.%.
Nr S-Z-C: normalized sand–silt–clay wt.%.

of the bedrock slab that previously occupied this scar (Fig. 4A). This failure probably was promoted by weathering fatigue of the slab because of progressive fracturing, chemical weathering, and syntectonic enhancement of relief. The actual failure event possibly was triggered by coseismic ground motion from a major earthquake along one of the three faults passing though this part of Owens Valley, as suggested by the known propensity of earthquakes to instigate rock avalanches (Keefer, 1984, 1994), the historic record of earthquakes as large as M = 8.3 in this part of Owens Valley, and the documented longer-term record of large earthquakes in Owens Valley obtained from the study of fault scarps (Lubetkin and Clark, 1988).

Upon failure, the frontal plate of the bedrock triangular facet moved as a rockslide down the 32° sloping detachment surface still exposed in the upper scar (Fig. 4A–B). The central part of this rockslide underwent continued failure by disaggregation, and was extensively disintegrated upon impacting the proximal piedmont at the base of the range front (Fig. 10A). Extensive disintegration combined with momentum caused this rock avalanche to transform to an inertial grain flow upon reaching the piedmont. By analogy with avalanches that have been observed, such as the one at Elm, Switzerland (Hsü, 1975), the North Long John rock avalanche probably progressed rapidly (50–100 km/h) downslope upon flow transformation, depositing the entire ~25 million m^3 of gravelly deposits as far as 1560 m from the range front during a few to tens of seconds. This short period included four phases of deposition indicated by the telescoped pattern between the three levee segments and the snout (Fig. 10B).

The surface of the rock avalanche deposits has been modified since emplacement by secondary processes (cf., Blair and McPherson, 1994a). Rilling from overland flow, caused by direct rainfall on the avalanche deposits, is most prevalent along the steep

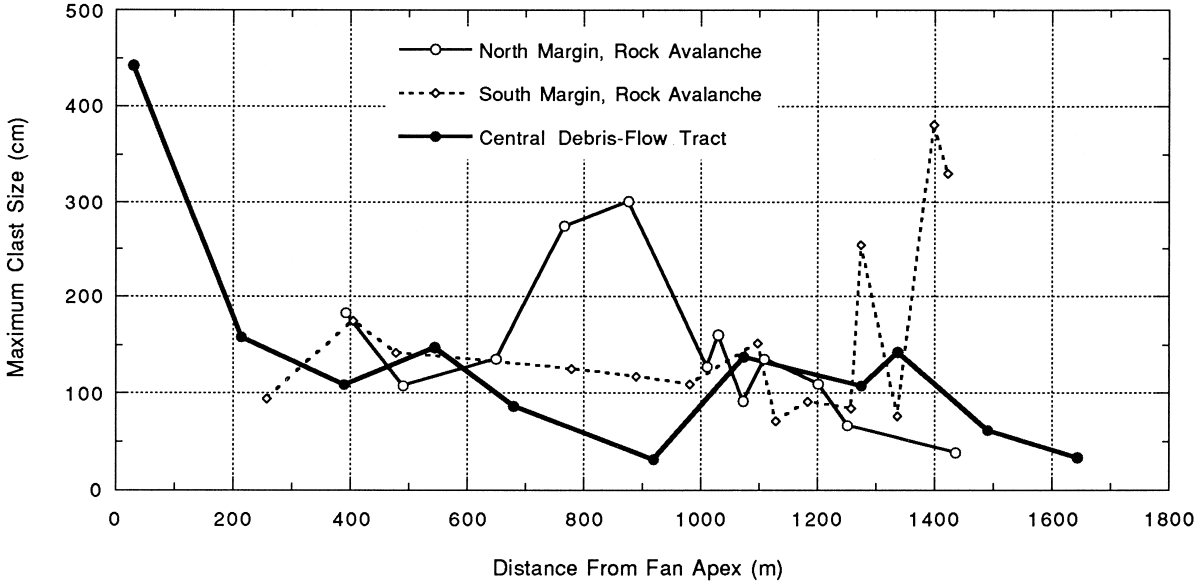

Fig. 9. Maximum clast size (d_1) for the northern and southern margins of the rock avalanche, and of the debris flow tracts plotted against radial position from the fan apex. No trends are apparent.

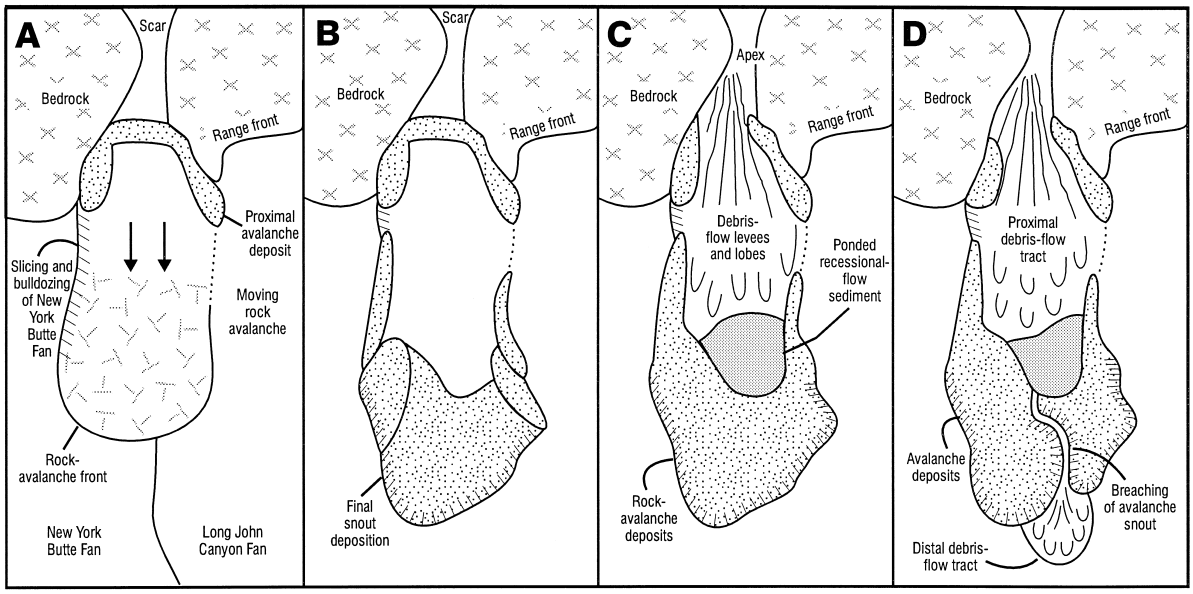

Fig. 10. Depositional history of North Long John fan shown by paleogeographic frames. (A) Fan initiation by rockslide failure of the range front bedrock facet. The central part of the slide disintegrates, and transforms to an inertial flow upon impact with the piedmont. The sole of the mass is sheared at the base of the range front, and the levee segments are deposited along the bedrock lining the outer scar. (B) Rock avalanche deposition is completed seconds later with the deposition of two additional levee segments and the snout 1.56 km from the range front. (C) Post-avalanche clast-rich debris flow levee and lobe deposition, and recessional flood 'pond' deposition, take place on the proximal fan. (D) Breaching of the avalanche snout subsequently occurs from overtopping, and the distal debris flow tract is initiated.

margins of the distal levees and snout (Fig. 4B). Overland flow from the catchment is responsible for the channeled breach through the snout deposits. Winnowing from rainsplash, overland flow, and wind erosion on the top of the avalanche deposits have produced a pebbly desert pavement layer one or a few clasts thick. Oxidation of clasts exposed at the surface have contributed to the development of a light to dark brown varnish. Accumulations of wind-blown sand also are present, especially on the snout of the rock avalanche where a 5 cm thick Av soil horizon is developed beneath the desert pavement. Translocation of finer sediment and iron oxides has resulted in the production of a 30 cm thick Bt soil horizon below the Av horizon (Fig. 7F). Desert plants cover about 30% of the avalanche surface, including xerophytes such as cattle spinach, desert holly, burroweed, creosote, and various grasses and cacti. Rodent burrows are locally common at the base of some of these plants, especially where they coincide with eolian deposits of sand.

The age of the North Long John rock avalanche deposition is uncertain, but several lines of evidence point to the earliest Holocene. The history of the complex post-avalanche pond and breached snout, the presence of gullies, desert pavement, a soil, and the partial burial by subsequent debris flows suggest that the avalanche event occurred many thousands of years ago. These and other characteristics of the North Long John avalanche deposits are similar to, or are less well developed than those of the nearby Blackhawk rock avalanche of Lucerne Valley, CA (Shreve, 1968, 1987). The Blackhawk event occurred about 20 Ka BP based on carbon-14 age determinations from snail shells collected from a back-snout pond. Unlike the North Long John avalanche, the Blackhawk avalanche has been cemented at the surface by calcite. Older avalanche deposits on the Blackhawk Canyon fan are notably better cemented, which indicates an increasing degree of cementation with age (Shreve, 1968, 1987). The lack of any cements, and the lighter desert varnish and less developed desert pavement, suggest that the North Long John avalanche was deposited much more recently than 20 Ka. Given these older and younger age constraints, the time of deposition of the North Long John rock avalanche is estimated at about 10 Ka BP.

The rock avalanche and subsequent debris flow deposits account for all of the volume of the fan catchment, indicating that a catastrophic avalanche initiated the North Long John fan and fan catchment system. This relatively recent ($\sim$10 Ka) age of initiation contrasts with the probable onset of the adjoining New York Butte and Long Canyon fans several million years earlier, during the nascent stage of Owens Valley development. Prior to the North Long John rock avalanche, the triangular bedrock facet that shed the avalanche was largely intact, and lacked a fan at its base. This pre-avalanche state likely was similar to the present state of the next triangular facet to the north, between the New York Butte and French Spring fan (Fig. 4A). Emplacement of the North Long John rock avalanche established the initial platform for this fan between the larger, previously coalesced New York Butte and Long Canyon fans. This event forced the feeder channel of the Long Canyon fan to lengthen 1 km to bypass the rock avalanche platform (Figs. 3 and 4C). The Long Canyon fan apex also was repositioned 1 km downslope, and 123 m lower in elevation.

5. Post-avalanche fan evolution

About 4 million m^3 of debris flow sediment accumulated on the North Long John fan since the rock avalanche, including deposits from the most recent debris flow of 22 August 1984 (Fig. 4C). This 1984 event resulted from colluvial slope failure instigated by strong, flashy thunderstorm precipitation in the catchment. This thunderstorm also triggered debris flows on other fans of the Inyo piedmont, including the Dolomite fan (Fig. 3; Blair and McPherson, 1998). Post-avalanche debris flow deposition on the North Long John fan dominantly has occurred in the proximal tract, where $\sim$3.7 million m^3 are found, compared to about 0.3 million m^3 of sediment for the distal tract (Fig. 4B–E). These deposits were described at 11 stations across the fan to characterize their facies and constituent forms (Fig. 5).

5.1. Forms and facies of the debris flow tracts

Three debris flow facies are differentiated based on textures, bedding, and forms. The first consists of unstratified, sandy, muddy, pebbly, cobbly, coarse to fine boulder gravel present in paired, radially aligned,

straight to sinuous levees 50 to 200 cm high and 50 to 100 cm wide (Fig. 11A–B). Clast concentration is high but inhomogeneous in these levees, with the most clast-rich part present along the outer margins, and the more matrix-rich sediment along the insides. Elongate boulders and cobbles display a preferred orientation either parallel or slightly oblique to both the direction of slope and the trend of the levees (Fig. 11B). This levee facies is well developed on the proximal fan outward from the apex, between the proximal rock avalanche levees. Radial slopes in this tract slightly lessen distally from 16° to 12° (Fig. 6A). The bowed-upward composite cross profile (Fig. 6D) has significant roughness because of 1–4 m of local relief caused by the distribution of levees (Fig. 11A). This facies also is present, though less well developed, on the 9° sloping upper end of the distal debris flow tract.

The second debris flow facies consists of clast-rich and clast- to matrix-supported, slightly bouldery, sandy, muddy, cobbly, fine to very coarse pebble gravel. These deposits are present in lobate forms 10–50 cm high, 3–10 m across, and extending many tens of meters in a radial trend (Fig. 11C–E). They comprise stacked beds of similar dimensions when viewed in vertical cuts (Fig. 11F). The most clast-rich and coarsest part of this facies fringe the lobe margins, where interlocked fine boulders and cobbles are concentrated (Fig. 11C). Elongate clasts in these outer zones have a preferred alignment parallel to the lobe margin, including a radial alignment along the sides and a slope-perpendicular alignment along the snouts. The inner zones are more pebble dominated and matrix-supported (Fig. 11D). Cuts reveal that the coarsest fraction in the lobe centers tend to be concentrated near the tops (Fig. 11E). The clast-rich outer margins of many of these lobes lack matrix, although matrix-sized sediment commonly is found nearby, drained outward from the lobes. Matrix-free, imbricated pebbles and cobbles also are present in shallow rills through or upon these lobes (Fig. 11E). This debris flow lobe facies is widely developed downslope from the levee-dominated zone on the proximal and distal fan tracts (Fig. 5). The boundary between the levees and lobes on the proximal fan is demarcated by a prominent slope inflection from 12° to 5°. This lobe facies has a steeper (7–8°) surface slope on the distal debris flow tract (Fig. 4E).

The third debris flow facies consists of matrix-supported, pebbly sandy mud and pebbly muddy sand deposited downslope from the proximal clast-rich lobe zone in the back-snout 'pond' (Figs. 5 and 7C). Where exposed, this facies consists of interbedded clast-poor units 5 to 20 cm thick. They contrast with the adjoining lobe facies by the presence of well-stratified clast-poor muddy beds, and by containing mudcracked silt layers. These beds are nearly horizontal, dipping downslope at $< 1°$.

To further characterize the debris flow tracts, maximum clast size (d_1) was determined at 11 study stations, and grain-size analysis was conducted on three samples. Maximum clast size varies from 33 to 442 cm, although most clasts are < 150 cm across (Fig. 9). The single largest clast, a fine-grained block with a d_1 of 442 cm, is present within a levee near the fan apex. Except for this clast, and the absence of boulders in the ponded area, the maximum clast size in the debris flow deposits is similar, irrespective of radial distance from the apex (Fig. 9). Boulder concentration, however, is significantly higher in the levee zones than in the lobe zones. The maximum values of clast size in the debris flows rival those of the rock avalanche facies, but show no correlation to them (Fig. 9). The finer fraction (< 1.6 cm or -4ϕ) of the debris flows was characterized by grain-size analysis of three samples representative of each facies, including NLJ-04 from a levee of the upper tract, NLJ-05 from the clast-poor deposits of the back-snout 'pond,' and NLJ-06 from a lobe deposit of the distal fan (Fig. 5). The proximal clast-rich levee and distal clast-rich lobe samples have a similar distribution of grain sizes, with a wide span of grades that average 28% pebbles, 9% granules, 29% sand, 25% silt, and 9% clay (Fig. 8; Table 1). Both of these samples are unsorted, with Folk Inclusive Graphic Standard Deviation (S_1) values of 4.37ϕ and 4.22ϕ. The clast-poor 'pond' sample contains less gravel and more sand than the clast-rich samples but still is extremely poorly sorted ($S_1 = 3.66\phi$), containing 14% pebbles, 4% granules, 47% sand, 29% silt, and 6% clay (Fig. 8; Table 1).

5.2. Reconstructed depositional processes

The debris flows of the North Long John fan originated through the destabilization of colluvial

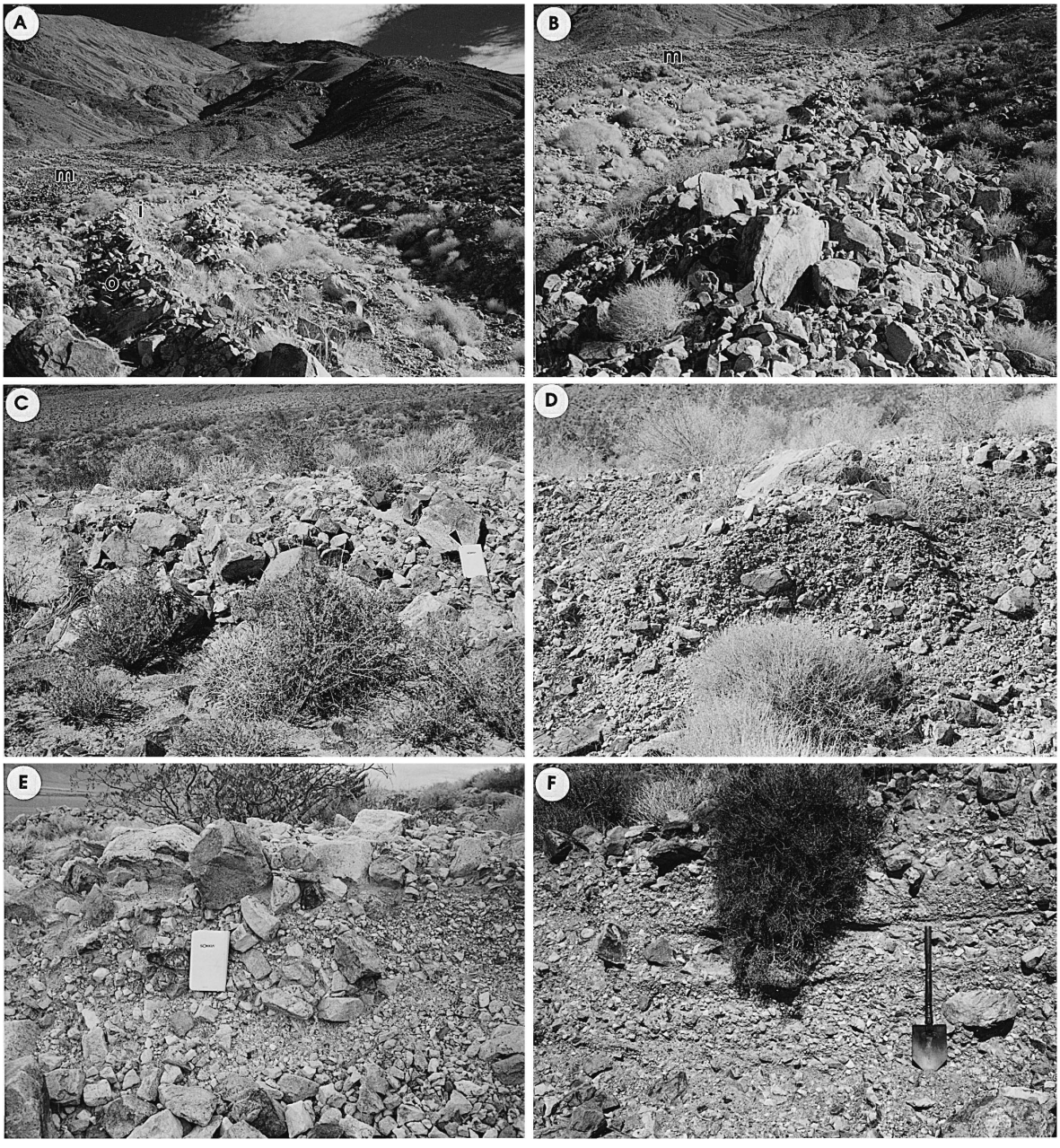

Fig. 11. Post-avalanche debris flow deposits on the North Long John fan. (A) Overview towards the fan apex of sinuous debris flow levees 1 to 2 m high. The rubbly, matrix-poor outer levee (o) contrasts with the more matrix-rich inner zone (i). Also marked is an older winnowed mantle (m). (B) View of a proximal fan levee with abundant cobbles and boulders displaying a preferred radial *a*-axis alignment. Also visible are the varnished mantle (m) on older debris flow deposits. (C) End of the 50 cm high margin of a clast-rich lobe on the proximal fan (at fieldbook, arrow). Interlocked angular cobbles are concentrated along this lobe margin. (D) Cut 1 m tall through the center of a proximal-fan lobe displaying an unorganized, matrix-supported, muddy, fine to coarse pebble gravel texture. (E) Vertical cut 1 m tall of the central part of a thick lobe of the distal debris flow tract revealing a clast- to matrix-supported, clast-rich, angular, muddy, cobbly, fine to coarse pebble gravel. The coarsest clasts are concentrated near the top. (F) Vertical cut 1.5 m tall of the distal debris flow tract containing at least five stacked beds of debris flows 10 to 20 cm thick. They consist of clast- to matrix-supported, clast-rich, angular, muddy, sandy, cobbly, fine to coarse pebble gravel divided by finer-grained clast-poor debris flows.

sediment mantling the rock avalanche scar that now serves as the nascent fan catchment (Fig. 4A). As exemplified by the 22 August 1984 event, these colluvial slopes are transformed into debris flows by the rapid addition of thunderstorm precipitation in the catchment (Fig. 4C). The North Long John fan catchment is the sole origin of these debris flows based on the source direction indicated by the conical shape of the debris flow tracts, and on the direct match in composition between the nearly monolithologic aplite clasts and the aplite bedrock unique to this catchment.

The texture, fabric, and radial orientation of the levees of the debris flow tracts are characteristics consistent with features observed to form from the passage of clast-rich and boulder-bearing surges of debris flows (Sharp, 1942; Sharp and Nobles, 1953; Johnson, 1970). The levees form as the outer margins of a passing front of a lobate surge, and undergo deposition after being sheared from the surge because of frictional drag along the sides (Sharp and Nobles, 1953; Johnson, 1984; Pierson, 1986). The radial fabric of the clast long axes originates as these coarse clasts first are lifted by differential buoyancy to the top of the moving flow, then conveyed to the front by the greater velocity of the upper flow tread resulting from frictional drag along the base, and then finally pushed laterally aside in a snow-plow-like fashion by the mass of the debris flow (Johnson, 1970; Pierson, 1980; Blair and McPherson, 1998).

The distinctive form, unsorted gravelly texture, and the fabric of the lobes that are present downslope from the leveed zones are typical of debris flow lobe deposits (Sharp and Nobles, 1953; Broscoe and Thomson, 1969). The concentration of the most clast-rich part of these lobes along the outer margins indicates that selective sorting of the more buoyant coarse clasts was taking place, first towards the lobe front, and then to the side margin (e.g., Blackwelder, 1928; Sharp and Nobles, 1953; Pierson, 1981). A key difference between the lobes and levees, besides morphology, is that the lobes overall lack boulder-sized clasts, whereas the levees are boulder-rich. The selective depletion of the boulder fraction from the moving debris flows causes a loss of lateral support, allowing them to expand into lobes (Blair and McPherson, 1998). This transition is reflected geomorphically on the North Long John fan by a change in surface slope from 12° to 5° (Fig. 5).

Another feature observed in the clast-rich debris flow facies of the North Long John fan is outward drainage of the matrix from the coarse margins immediately upon levee or lobe deposition. This process initiates the boulder and cobble mantles common on the upper fan (Fig. 7D). Matrix draining indicates that either this matrix had low cohesive strength, or that the clasts were not adequately interlocked to effectively contain the fines. Interlocking may be difficult for the North Long John fan debris flows because the clasts, all derived from the avalanche scar, are angular and typically equant in shape. The softness of the matrix also denotes that it has low cohesive strength, especially when compared to debris flows on other Inyo piedmont fans (Blair and McPherson, 1998). This contrast in matrix cohesion may result from differences in the weathering products of the catchments because of variable bedrock lithology. Probably a more important factor is that the North Long John matrix formed cataclastically during the rock avalanche, rather than through chemical weathering typical of the neighboring fan catchments. This cataclastic origin has produced a suite of clay-sized sediment consisting of minute fragments of the minerals making up the aplite, instead of a collection of clay minerals produced through chemical alterations, and possessing clay mineral properties such as adhesion and crystal anisotropy.

The more mud-dominated, clast-poor, debris flow facies in the back-snout ‘pond’ of the North Long John fan is interpreted as the trapped, less viscous, clast-poor phase of debris flows, as well as the deposits of sediment-rich flows of recessional water that have winnowed the debris flows. Observations of debris flows on fans indicate that a clast-poor debris flow stage followed by recessional flood water flow are common (Sharp and Nobles, 1953; Pierson, 1981, 1986; Johnson, 1984; Blair and McPherson, 1998). Recessional water flows result from continued drainage from the catchment of overland flow not significantly charged with sediment. The key affect of recessional water flow is the selective fine-fraction winnowing of the poorly sorted debris flow material, and the movement of this sediment into the back-snout pond. This recessional flow

facies is developed in the proximal part of the North Long John fan, instead of on the distal fan, because of the damming effect of the rock avalanche deposits.

The grain-size data of the < 1.6 cm ($< -4\phi$) fraction provide some important insight to the relationship between the North Long John rock avalanche and the subsequent debris flows. This fraction in the debris flows is generally similar to that of the rock avalanche, including an unsorted distribution of size grades (Fig. 8). The key differences are that the samples from the rock avalanche contain a higher percentage of gravel (60% vs. 20 to 40%) and have significantly less mud (12% vs. 33%; Fig. 8B–F). These differences are represented in the cumulative curves by a well-shaped arcuate distribution of samples from the rock avalanche, and an irregular linear pattern for the samples form the debris flows, which especially diverge from the rock avalanche pattern in the mud fraction (Fig. 8A). The cumulative curve in the mud fraction (finer than 4ϕ) for the debris flow samples have an identical plot, regardless of facies (Fig. 8A). Given that the debris flow deposits are derived either from the cataclastic material accumulated along the avalanche scar or, in the case of the distal fan by partial reworking of the avalanche snout deposits, the overall similarities in the size suite is expected. The enrichment in mud in the debris flow samples, however, shows that this fraction was selectively concentrated by the debris flow process. This enrichment in the mud fraction probably is indicative of the critical mud concentration needed for the initiation of a debris flow given the overall texture of the cataclastic colluvium.

The surface of the North Long John debris flow deposits has been modified by secondary processes. Foremost amongst these is the fine-fraction winnowing of sediment by overland flows, aided by rainsplash and wind erosion, to produce a matrix-free, surface gravel lag. This winnowing process occurs during recessional water flow of a debris flow event, and during rainfall-triggered overland flows. The most widespread product of this winnowing process is the development of a boulder–cobble mantle or pavement one or more clasts thick (Fig. 7D), a feature also noted on the surface of the nearby Trollheim fan in Deep Springs Valley, CA (Blair and McPherson, 1992). The presence of drained matrix from the lobes of North Long John fans suggests that the development of this mantle is initiated by matrix drainage, and then advanced by subsequent secondary water winnowing. Overland flow from the fan catchment also is responsible for the development of the incised channel through the rock avalanche snout that leads to the debris flow tract of the distal fan. Other prominent secondary processes on the debris flow surfaces include oxidation of clasts, and the growth of desert bushes and grasses.

5.3. Reconstructed post-avalanche depositional history

The proximal debris flow tract post-dates deposition of the rock avalanche, given that it is derived from colluvium mantling the avalanche scar, and that it has partially buried avalanche deposits (Fig. 4A–B). Deposition of this tract commenced upon the development of the colluvial mantle in the nascent catchment, which accumulated as rockfall of the loose bedrock fragments granulated along the avalanche scar. These colluvial particles were cataclastically formed during the rock avalanche through pulverization as the frontal bedrock facet slid along the detachment surface. Observations from historical events indicate that such rockfall colluvium ('afterfall') accumulates within weeks to months of the event (Hadley, 1978; Blair and McPherson, 1994b). The transformation of this colluvial material in the North Long John fan catchment to a debris flow awaited favorable flashy precipitation in the catchment, precipitation known in Owens Valley to result from summer thunderstorms (Beaty, 1970; Blair and McPherson, 1998). The infrequency of such precipitation in a given catchment dictates that the proximal North Long John fan debris flow tract aggraded sporadically through time from rare storms, with secondary surface processes affecting sedimentation between storms. Debris flows instigated since the avalanche event have deposited as much as 20 m of clast-rich levees and lobes in this proximal fan tract, whereas the more mobile, recessional clast-poor debris flows and water flows accumulated within the ~ 6 m deep trap behind the rock avalanche snout (Fig. 10C). This trap eventually filled to the level of the snout (Fig. 7C–D).

Deposition of debris flows on the distal fan tract commenced upon breaching of the rock avalanche snout by a channel that connects the proximal and distal debris flow tracts (Fig. 10D). This breach likely occurred once the back-snout pond had filled with recessional debris flow material from the proximal tract, after which time flows overtopped the snout. Once initiated, downcutting of the sinuous snout-bypass channel probably was rapid because of the uncemented, homogeneous texture of the avalanche material in the snout. This theory of downcutting by overtopping is supported by the location of this incised channel at the topographically lowest point through the snout (Fig. 4B and Fig. 7C). With the development of this avalanche-bypass channel, debris flows could proceed from the fan apex to the distal debris flow tract, as did the 22 August 1984 debris flow (Fig. 4C). Some of the debris flow deposits of the distal tract also were derived from the avalanche snout during incision of the bypass channel. The lack of darkly varnished pavements on the debris flow deposits of the distal tract, in contrast to the proximal tract (cf. Fig. 3E and Fig. 7D), supports a more recent age of development of the distal tract. This relative age also is suggested by the low volume of sediment found on the distal tract.

The abundance of colluvium upon the steep slopes of the North Long John fan catchment indicates that debris flows will continue to be instigated given favorable input of flashy thunderstorm precipitation. Aggradation of the proximal tract will lead to progradation of the debris flow levee and lobe facies belts, and to further burial of the rock avalanche deposits. Breaching of the avalanche snout allows future clast-rich lobes and recessional stage deposition to continue reaching and aggrading the distal tract, thereby lengthening the fan radius.

6. Comparison with adjoining mature piedmont fans and fan catchments

The North Long John fan and catchment have morphometric characteristics that significantly differ from the adjoining New York Butte and Long Canyon systems. The New York Butte and Long Canyon fan catchments have respective areas of 9.9 and 19.5 km^2, relief of 1713 to 1911 m, and well-developed, dense drainage nets of fourth- and fifth-order feeder channels (Figs. 3 and 4A). These attributes contrast with the 2.0 km^2 area, 1065 m relief, and second-order feeder channel of the North Long John catchment. Relief ratios (catchment relief / $\sqrt{\text{area}}$) are 0.54 and 0.43, respectively, for the New York Butte and Long Canyon fan catchments, vs. 0.75 for the North Long John fan catchment.

The 0.8 km^2 area of the North Long John fan is notably smaller than the 2.0 and 4.3 km^2 areas of the adjoining New York Butte and Long Canyon fans, which also have significantly longer radii (2.4 and 2.8 km long, respectively) than the 1.7 km long radius of the North Long John fan. The average slope of 8.8° for the North Long John fan is steeper than the 6 to 7° average slopes of the adjoining fans. The slope of the North Long John fan also differs from its relatively smooth-surfaced conical neighbors by having a more irregular composite morphology resulting from the presence of rock avalanche deposits and two debris flow tracts. The adjoining fans are smoother because they are continuously underlain by clast-rich debris flow lobes, and because they contain surfaces of well-developed and deeply varnished desert pavement. These differences between the North Long John fan vs. the New York Butte and Long Canyon fans, and between the respective catchments, are the result of the nascent stage of development of the North Long John system (Stage 1 of Blair and McPherson, 1994a) compared to the older and more mature development of the adjoining fans of the Inyo Mountains piedmont.

7. Implications

The key implication of the study of the North Long John fan is that not all fans of a particular piedmont are of the same longevity or stage of development. This is especially true of fans developed from the range front bedrock triangular facets dividing more mature fan catchments. Instability of these triangular bedrock facets with time promotes failure, perhaps by the initiation of rock avalanches, that leave colluvium-lined scars ideal for subsequent fan depositional events. This study also points out

that the geological hazards on the piedmont beneath triangular bedrock facets (rockfalls, rockslides, and rock avalanches) contrast with the dominantly debris flow or water-flood hazards of the more mature fans. Differences in the relative ages of adjoining fans also lead to complications for the common practice of mapping relative-aged surfaces on piedmonts. This study demonstrates that complications arise from differences in the timing of fan initiation, and with the degree of diachroneity of fan provinces.

The North Long John fan case study also has implications for the stratigraphic record of piedmonts. Differentiating the deposits of ancient piedmonts are complicated because a new fan can be initiated much later than other fans. The stratigraphic signature of this phenomenon for the North Long John fan would be the sharp accumulation of megabrecciated rock avalanche deposits above the coalesced tips of older and larger fans, followed by debris flow deposits with especially angular clasts of a monolithologic composition. The peculiar occurrence of recessional flood 'pond' facies in the proximal fan area also would be an important indicator of the presence of a rock avalanche barrier directly downfan.

8. Conclusions

The North Long John alluvial fan was initiated by a large rock avalanche triggered by the collapse of a former bedrock triangular facet. The rock avalanche provided the initial sediment of the nascent fan, and left a large, spoon-shaped scar in the range front stocked with cataclastically generated muddy and gravelly colluvium. Thus, this rock avalanche served as an alluvial fan 'starter kit.' Thunderstorm-induced debris flows generated from the catchment subsequent to rock avalanche emplacement have built proximal and distal debris flow tracts that partially bury the rock avalanche. This process will continue because of the abundance of mud-bearing sediment upon the steep catchment slopes, and the likely continued occurrence of thunderstorms in Owens Valley. The nascent stage of the North Long John fan contrasts with the more mature, larger neighboring fans of the Inyo Mountains piedmont.

Acknowledgements

Two anonymous reviewers kindly provided critiques that improved this manuscript. Blair & Associates is thanked for research support.

References

Beaty, C.B., 1970. Age and estimated rate of accumulation of an alluvial fan White Mountains, California. American Journal of Science 268, 50–77.

Blackwelder, E., 1928. Mudflow as a geologic agent in semi-arid mountains. Geological Society of America Bulletin 39, 465–484.

Blair, T.C., McPherson, J.G., 1992. The Trollheim alluvial fan and facies model revisited. Geological Society of America Bulletin 104, 762–769.

Blair, T.C., McPherson, J.G., 1994a. Alluvial fan processes and forms. In: Abrahams, A.D., Parsons, A. (Eds.), Geomorphology of Desert Environments. Chapman & Hall, London, pp. 354–402.

Blair, T.C., McPherson, J.G., 1994b. Alluvial fans and their natural distinction from rivers based on morphology, hydraulic processes, sedimentary processes, and facies. Journal of Sedimentary Research A 64, 451–490.

Blair, T.C., McPherson, J.G., 1998. Recent debris-flow processes and resultant form and facies of the Dolomite alluvial fan Owens Valley, California. Journal of Sedimentary Research 68, 800–818.

Blair, T.C., McPherson, J.G., 1999. Grain-size and textural classification of coarse sedimentary particles. Journal of Sedimentary Research 69, 6–19.

Broscoe, A.J., Thomson, S., 1969. Observations on an alpine mudflow, Steele Creek, Yukon. Canadian Journal of Earth Sciences 6, 219–229.

Bull, W.B., 1984. Tectonic geomorphology. Journal of Geological Education 32, 310–324.

Burchfiel, B.C., 1966. Tin Mountain landslide, southeastern California, and the origin of megabreccia. Geological Society of America Bulletin 77, 95–100.

Fauque, L., Strecker, M.R., 1988. Large rock avalanche deposits (Strurzstrome, sturzstroms) at Sierra Aconquija, northern Sierras Pampeanas, Argentina. Eclogae Geologicae Helvetiae 81, 579–592.

Folk, R.L., 1974. Petrology of Sedimentary Rocks. Hemphill Publishing, Austin, TX.

Gates, W.B., 1987. The fabric of rockslide avalanche deposits. Bulletin of the Association of Engineering Geologists 24, 389–402.

Hadley, J.B., 1964. Landslides and related phenomena accompanying Hebgen Lake earthquake of August 17, 1959. U.S. Geological Survey Professional Paper 435, 107–138.

Hadley, J.B., 1978. Madison Canyon rockslide, Montana, U.S.A. In: Voight, B. (Ed.), Rockslides and Avalanches, Vol. 1. Elsevier, Amsterdam, pp. 167–196.

Hollett, K.J., Danskin, W.R., McCaffrey, W.H., Walti, C.L., 1991. Geology and water resources of Owens Valley, California. U.S. Geological Survey Water-Supply Paper 2370-B, 77 pp.

Horton, R.E., 1945. Erosional development of streams and their drainage basins; hydrophysical approach to quantitative morphology. Geological Society of America Bulletin 56, 275–370.

Hsü, K.J., 1975. Catastrophic debris streams (Sturzstroms) generated by rockfalls. Geological Society of America Bulletin 86, 129–140.

Johnson, A.M., 1970. Formation of debris flow deposits. In: Johnson, A.M. (Ed.), Physical Processes in Geology. Freeman, Cooper, San Francisco, pp. 433–448.

Johnson, A.M., 1984. Debris flow. In: Brunsden, D., Prior, D.B. (Eds.), Slope Instability. Wiley, New York, pp. 257–361.

Keefer, D.K., 1984. Rock avalanches caused by earthquakes: source characteristics. Science 223, 1288–1290.

Keefer, D.K., 1994. The importance of earthquake-induced landslides to long-term slope erosion and slope-failure hazards in seismically active regions. Geomorphology 10, 265–284.

Lubetkin, L.K.C., Clark, K.M., 1988. Late Quaternary activity along the Lone Pine fault, eastern California. Geological Society of America Bulletin 100, 755–766.

Pakiser, L.C., 1960. Transcurrent faulting and volcanism in Owens Valley, California. Geological Society of America Bulletin 71, 153–160.

Pakiser, L.C., Kane, M.F., Jackson, W.H., 1964. Structural geology and volcanism of Owens Valley region, California—A geophysical study. U.S. Geological Survey Professional Paper 438, 65 pp.

Pierson, T.C., 1980. Erosion and deposition by debris flows at Mt. Thomas, North Canterbury, New Zealand. Earth Surface Processes 5, 227–247.

Pierson, T.C., 1981. Dominant particle support mechanisms in debris flows at Mt. Thomas, New Zealand, and implications for flow mobility. Sedimentology 28, 49–60.

Pierson, T.C., 1986. Flow behavior of channelized debris flows, Mount St. Helens, Washington. In: Abrahams, A.D. (Ed.), Hillslope Processes. Allen and Unwin, Boston, pp. 269–296.

Ross, D.C., 1967. Generalized geologic map of the Inyo Mountains region, California. U.S. Geological Survey Map 1–506.

Sharp, R.P., 1942. Mudflow levees. Journal of Geomorphology 5, 222–227.

Sharp, R.P., Nobles, L.H., 1953. Mudflow of 1941 at Wrightwood, southern California. Geological Society of America Bulletin 64, 547–560.

Shreve, R.L., 1968. The Blackhawk landslide. Geological Society of America Special Paper 108, 47 pp.

Shreve, R.L., 1987. Blackhawk landslide, southwestern San Bernardino County, California. Geological Society of America Centennial Field Guide Cordilleran Section, pp. 109–114.

Strahler, A.N., 1964. Quantitative geomorphology of drainage basins and channel networks. In: Chen, V.T. (Ed.), Handbook of Applied Hydrology. McGraw-Hill, New York, pp. 40–74.

Streitz, R., Stinson, M.C., 1974. Geologic map of the 1:250,000 scale Death Valley sheet, California. California Division of Mines and Geology, Sacramento.

Wallace, R.E., 1978. Geometry and rates of change of fault-generated range fronts, north-central Nevada. U.S. Geological Survey Journal of Research 5, 637–650.